Published in final edited form as:
Cancer Res. 2005 August 1; 65(15): 6711–6718. doi:10.1158/0008-5472.CAN-05-0310.

Increased Tumorigenicity and Sensitivity to Ionizing Radiation upon Loss of Chromosomal Protein HMGN1

Yehudit Birger[1], **Frédéric Catez**[1], **Takashi Furusawa**[1], **Jae-Hwan Lim**[1], **Marta Prymakowska-Bosak**[1], **Katherine L. West**[1], **Yuri V. Postnikov**[1], **Diana C. Haines**[2], and **Michael Bustin**[1]

[1]Protein Section, Laboratory of Metabolism, Center for Cancer Research, National Cancer Institute, NIH, Bethesda, Maryland [2]Pathology/Histotechnology Laboratory, Science Applications International Corporation, National Cancer Institute, Frederick, Maryland

Abstract

We report that loss of HMGN1, a nucleosome-binding protein that alters the compaction of the chromatin fiber, increases the cellular sensitivity to ionizing radiation and the tumor burden of mice. The mortality and tumor burden of ionizing radiation–treated *Hmgn1*$^{-/-}$ mice is higher than that of their *Hmgn1*$^{+/+}$ littermates. *Hmgn1*$^{-/-}$ fibroblasts have an altered G_2-M checkpoint activation and are hypersensitive to ionizing radiation. The ionizing radiation hypersensitivity and the aberrant G_2-M checkpoint activation of *Hmgn1*$^{-/-}$ fibroblasts can be reverted by transfections with plasmids expressing wild-type HMGN1, but not with plasmids expressing mutant HMGN proteins that do not bind to chromatin. Transformed *Hmgn1*$^{-/-}$ fibroblasts grow in soft agar and produce tumors in nude mice with a significantly higher efficiency than *Hmgn1*$^{+/+}$ fibroblasts, suggesting that loss of HMGN1 protein disrupts cellular events controlling proliferation and growth. *Hmgn1*$^{-/-}$ mice have a higher incidence of multiple malignant tumors and metastases than their *Hmgn1*$^{+/+}$ littermates. We suggest that HMGN1 optimizes the cellular response to ionizing radiation and to other tumorigenic events; therefore, loss of this protein increases the tumor burden in mice.

Introduction

Chromatin plays a central role in regulating the fidelity of gene expression, in maintaining genomic stability, and in mounting proper responses to various cellular stresses, including UV and ionizing radiation (1). For example, the repair of irradiation-induced double-strand breaks (DSB) is linked to the phosphorylation of the histone variant H2AX (2), and the loss of a single *H2ax* allele decreases genomic stability and increases tumor susceptibility (3, 4). Additional histone modifications, such as methylation and acetylation, were also found to play important roles in DNA repair processes (1) and inhibitors of histone deacetylases are being tested as potential anticancer therapeutic agents (5). The transcription regulatory function of the tumor suppressor p53, which plays a key role in determining cellular stability and transformation, is dependent on specific binding to chromatin (6); moreover, chromatin

Requests for reprints: Michael Bustin, Protein Section, Laboratory of Metabolism, Center for Cancer Research, National Cancer Institute, NIH, Building 37, Room 3122B, 9000 Rockville Pike, Bethesda, MD 20892. Phone: 301-49605234; bustin@helix.nih.gov..

All animals were cared for and used humanely according to the U.S. Public Health Service Policy on Humane Care and Use of Animals (2000); the *Guide for the Care and Use of Laboratory Animals* (1996); and the U.S. Government Principles for Utilization and Care of Vertebrate Animals Used in Testing, Research, and Training (1985). National Cancer Institute-Frederick animal facilities and animal program are accredited by the Association for Assessment and Accreditation of Laboratory Animal Care International.

remodeling complexes, such as BRG1 and BRM, play a role in genomic stability (7). Perturbation in the higher-order chromatin structure has also been linked to the activation of the ATM, a protein kinase that plays a key role in the cellular response to ionizing radiation and the prevention of tumor formation (8, 9). Likewise, numerous studies have linked the correct repair of UV damage to the ability of nucleotide excision repair complexes to reach the UV-damaged sites in chromatin (10–12). Thus, the structure of chromatin and the ability of nuclear complexes that sense and repair DNA damage to reach their target sites in chromatin play an important role in DNA repair, in maintaining genomic stability, and in tumor susceptibility (13).

Given that access of regulatory factors and DNA repair complexes to their target sites in chromatin is important, it is possible that nuclear proteins, such as the nonhistone HMGN proteins (14, 15), that are known to affect the stability of the higher-order chromatin structure may play a role in DNA repair processes and in tumorigenicity. The high mobility group N (HMGN) is a family of structural proteins present in the nuclei of all mammalian cells that binds specifically to nucleosomes, the building block of the chromatin fiber (14, 15). HMGN proteins move rapidly throughout the nucleus, bind to nucleosomes transiently (16, 17), and reduce the compaction of the chromatin fiber (14, 15). The binding of HMGN proteins to nucleosomes affects the levels of posttranslational modification in core histones and alters DNA-related nuclear processes such as transcription (18–20) and replication (21). *Hmgn1*$^{-/-}$ mice are hypersensitive to UV most likely because loss of HMGN1 protein alters the accessibility of the damaged sites to the nucleotide excision repair machinery and decreases the rate of removal of UV-induced lesions from transcriptionally active chromatin (22). These findings, and the growing evidence that chromatin plays an important role in DSB repair, led us to test whether HMGN1 affects the cellular response to ionizing radiation.

Using *Hmgn1*$^{-/-}$ mice and cells, we find that HMGN1 protein plays a role in the cellular ability to mount a proper response to ionizing radiation and that loss of this protein increases the tumor susceptibility in mice. Ionizing irradiation leads to accelerated tumor formation and death of mice lacking HMGN1 protein, compared with wild-type mice. Likewise, *Hmgn1*$^{-/-}$ fibroblasts are hypersensitive to ionizing radiation and fail to arrest properly in G_2-M phase of the cell cycle. SV40-transformed *Hmgn1*$^{-/-}$ fibroblasts grow in soft agar and produce tumors in nude mice with a significantly higher efficiency than SV40-transformed *Hmgn1*$^{+/+}$ fibroblasts, suggesting that loss of HMGN1 protein disrupts cellular events controlling proliferation and growth. *Hmgn1*$^{-/-}$ mice have a higher incidence of multiple malignant tumors and metastases than wild-type mice.

Our results identify a chromatin-binding protein that plays a role in the cellular response to ionizing radiation and indicate that loss of HMGN1 impairs the cellular response to ionizing radiation and increases susceptibility to tumor formation.

Materials and Methods

Animals and cell lines

Hmgn1$^{-/-}$ mice, primary mouse embryonic fibroblasts (MEF), MEF-derived cell lines, and SV40-transformed MEF cells, expressing either wild-type or mutant HMGN1 protein, under the control of the Tet promoter, were generated and characterized as described elsewhere (22). Mice were backcrossed for at least six generations and were over 95% pure. Primary MEFs were used up to passage 5 because older MEFs had an altered phenotype. The longevity study was terminated after 112 weeks at which all surviving mice were sacrificed.

Assessment of genomic instability

Cells were incubated with 0.05 μg/mL colcemid for 1.5 hours, treated with 0.7% KCl for 5 minutes at room temperature, fixed for 16 hours at 4°C with in a solution of 3:1 methanol/acetic acid, spread on slides, and stained with Giemsa as recommended by the manufacturer.

Irradiation of animals

A total of 40 mice (20 each of *Hmgn1*$^{-/-}$ and *Hmgn1*$^{+/+}$ littermates), 6 to 8 weeks old, were γ-irradiated using a ^{137}Cs Shepherd Mark II irradiator, with a cumulative dose of 9 Gy (3 Gy, thrice, on alternating days). The animals were monitored for 12 months after irradiation for appearance of tumors and survival and then sent to necropsy.

Injection of cells into NU/NU mice

Twenty immunodeficient nude (nu/nu) female mice were injected s.c., in two separate experiments, with either 2×10^6 *Hmgn1*$^{-/-}$ or 2×10^6 *Hmgn1*$^{+/+}$ transformed MEFs or with PBS. The animals were monitored for tumor formation for 10 weeks and than sent to necropsy. In animals that developed tumors, no metastases were found within the 10 weeks of observation. The experiment was done twice.

Irradiation and survival of mouse embryonic fibroblasts

Cells (5×10^4) were plated in 35 mm dishes a day before their irradiation. The cells were exposed to ionizing radiation from a ^{137}Cs Shepherd Mark II irradiator at the indicated doses. Fresh medium was added to the plates immediately after irradiation and survival was determined 72 hours after treatment. The surviving cells were counted by trypan blue exclusion and survival was expressed as a percentage using untreated cells as the 100% value. The experiments were conducted in triplicates and were repeated at least twice.

Evaluation of spontaneous tumor formation

Hmgn1$^{+/+}$ males and females (24 and 22, respectively) and *Hmgn1*$^{-/-}$ males and females (24 and 22, respectively) were followed. Dead or ill mice were subjected to histopathologic examination. More than 40 tissues were sectioned, stained with H&E, and analyzed.

Cell cycle analysis

Cells (2×10^6-4×10^6) were fixed in 70% ethanol, washed in PBS/Triton/bovine serum albumin buffer, treated with anti–H3-P monoclonal antibody (Upstate, Charlottesville, VA). Following secondary antibody addition, the cells were treated with 100 units of RNase for 20 minutes at room temperature and stained with propidium iodide (20–50 μg/mL). The number of cells in mitosis (H3 phosphorylation) and the distribution of the cells in the different stages of the cell cycle was determined by fluorescence-activated cell sorting (FACS).

Soft agar growth and cell proliferation analysis

Six milliliters of 0.5% agar (42°C), suspended in DMEM with 10% fetal bovine serum, were poured into 10 cm Petri dishes and allowed to solidify. One milliliter of cells at different concentrations were mixed with 2 mL of the same agar suspension (42°C) and immediately layered over the hardened agar. The dishes were cultured at 37°C in 5% CO_2, with high humidity, for 3 to 5 weeks until colonies were visible and could be counted. Cell proliferation analysis were done in triplicates and repeated at least thrice.

Protein isolation and Western blot analysis

H2AX phosphorylation was determined by Western blot analysis (antibody from Upstate). Cells were washed in PBS and sedimented at 600 × *g* for 10 minutes. The pellet was dissolved in 0.2 mol/L H_2SO_4 containing a protease inhibitor cocktail (Roche, Indianapolis, IN), vortexed with glass beads for 2 minutes, kept on ice for 5 minutes, and sedimented at 3,000 × *g* for 10 minutes. The supernatant was made 25% in TCA by adding 100% TCA, incubated on ice for 15 minutes, and sedimented at 3,000 × *g* for 20 minutes. The pellet was stored at −20°C overnight in 100% ethanol, air-dried, and resuspended with 50 to 100 μL of water. Proteins were resolved on 15% Tris-glycine-SDS gels, transferred to a polyvinylidene difluoride membrane, and subjected to Western blots.

Laser scissors

Double-stranded DNA breaks were induced along a defined path essentially as described before (23, 24). Briefly, 20 minutes before UV exposure, cells were treated with HOECHST 33258 (10 μg/mL). UV exposures were set on a Zeiss LSM 510 confocal microscope in a controlled temperature environment. Cells were exposed to a 364 nm laser along a predefined path, under a 40× C-apo lens. Cells were kept at 37°C for 10 to 30 minutes, fixed with 4% paraformaldehyde, and immunostained (25).

Statistical analyses

Statistical analyses were done using Fisher's two-sided test at 95% confidence.

Results

Increased carcinogenesis in irradiated *Hmgn1*$^{-/-}$ mice

To test whether loss of HMGN1 protein affects the susceptibility to radiation-induced carcinogenesis, we treated *Hmgn1*$^{-/-}$, *Hmgn1*$^{+/+}$, and *Hmgn1*$^{+/-}$ littermate mice with a sublethal schedule of γ-irradiation (ionizing radiation). Within 1 year of ionizing radiation treatment, only 45% of the *Hmgn1*$^{-/-}$ mice, compared with over 75% of their *Hmgn1*$^{+/+}$ littermates, survived, an indication that loss of HMGN1 protein decreased the survival rate of the irradiated mice (Fig. 1*A*). The 1-year survival rate of irradiated *Hmgn1*$^{+/-}$ mice (49%) was similar to that of the irradiated *Hmgn1*$^{-/-}$ mice, whereas the 1-year survival rate of nonirradiated mice (over 85%) was the same for *Hmgn1*$^{-/-}$ and their *Hmgn1*$^{+/+}$ littermates (data not shown). Tumors were detected in over 90% of all the mice that died within 1 year after irradiation. Necropsy revealed the presence of large thymic masses, which histologic examination confirmed to be lymphomas. Thus, loss of HMGN1 protein increased the incidence of lymphomas and the mortality of γ-irradiated mice.

Increased radiation sensitivity in *Hmgn1*$^{-/-}$ embryonic fibroblasts

To further test the role of HMGN1 in the cellular sensitivity to γ-irradiation, we prepared MEFs from day 13.5 *Hmgn1*$^{-/-}$, *Hmgn1*$^{+/+}$, and *Hmgn1*$^{+/-}$ embryos and measured their survival rate after exposure to various doses of ionizing radiation. The *Hmgn1*$^{-/-}$ cells were the most sensitive, with a D_{50} (irradiation dose resulting in 50% survival) of 3.5 Gy compared with a D_{50} of >7 Gy for *Hmgn1*$^{+/+}$ MEFs (Fig. 1*B*). The survival rate of the *Hmgn1*$^{+/-}$ cells was intermediate between that of the *Hmgn1*$^{+/+}$ and *Hmgn1*$^{-/-}$ MEFs, suggesting a dose-dependent function of HMGN1 protein in enhancing the cellular ability to survive ionizing radiation (Fig. 1*B*). Thus, in both whole animals and cell culture, loss of HMGN1 protein correlated with increased sensitivity to ionizing radiation.

To verify that increased sensitivity to ionizing radiation in the *Hmgn1*$^{-/-}$ MEFs is directly linked to loss of HMGN1 protein, we established stable revertant *Hmgn1*$^{-/-}$ MEFs,

expressing wild-type HMGN1 protein under the control of the inducible tetracycline response element promoter (i.e., the cells were *Hmgn1*$^{-/-}$ Tet$^{+/+}$). We already showed that in these cells, induction of the tetracycline response element promoter by doxycycline gradually increases the cellular levels of the HMGN1 protein until they are comparable with those present in wild-type cells (22, 26). We grew these *Hmgn1*$^{-/-}$ Tet$^{+/+}$ MEFs for 48 hours in either the presence or absence of doxycycline and then exposed the cells to various levels of γ-irradiation. Induction of HMGN1 expression by doxycycline (Fig. 1*D*) elevated the D_{50} values of cells from 4.0 to >9 Gy (Fig. 1*C*). Thus, reexpression of wild-type HMGN1 in the *Hmgn1*$^{-/-}$ cells decreased the cellular sensitivity to ionizing radiation and restored the survival of the cells to a level close to those of the wild-type *Hmgn1*$^{+/+}$ cells (compare Fig. 1*B* and *C*). Control experiments indicated that addition of doxycycline to nontransfected *Hmgn1*$^{-/-}$ or *Hmgn1*$^{+/+}$ cells did not affect their sensitivity to ionizing radiation (not shown). Thus, the hypersensitivity of the *Hmgn1*$^{-/-}$ to ionizing radiation is directly linked to the absence of HMGN1 protein.

The primary binding target of HMGN1 in the nucleus is the nucleosome (i.e., the fundamental building block of the chromatin fiber). To test whether the effects of HMGN1 on the cellular sensitivity to ionizing radiation are related to these chromatin interactions, we generated *Hmgn1*$^{-/-}$ *Tet*$^{+/+}$ cells expressing the double point mutant S20,24E-HMGN1, which bears two negative charges in the nucleosomal binding domain of the protein, and therefore does not bind to chromatin (25). In contrast to the cells expressing the wild-type protein, expression of the S20,24E-HMGN1 mutant (Fig. 1*D*) did not affect the cellular sensitivity to ionizing radiation and the D_{50} of the doxycycline-treated cells remained significantly lower than those of the *Hmgn1*$^{+/+}$ cells (Fig. 1*C*). Thus, the hypersensitivity of the *Hmgn1*$^{-/-}$ cells to ionizing radiation is linked to the inability of the HMGN1 protein to bind to chromatin. Therefore, we conclude that HMGN1 enhances the ability of a cell to survive ionizing radiation through its interaction with nucleosomes.

HMGN1 affects the G_2-M checkpoint

One of the earliest cellular responses to ionizing radiation that could be linked to chromatin is the phosphorylation of the histone variant H2AX (γ-H2AX; ref. 2). Because HMGN1 is a chromatin-binding protein, we tested whether loss of chromosomal protein HMGN1 affects H2AX phosphorylation. We plated a mixture of *Hmgn1*$^{+/+}$ and *Hmgn1*$^{-/-}$ cells on a microscope plate, induced DNA DSBs in a defined path within their nuclei with a UV laser beam, and visualized the accumulation of phosphorylated H2AX in the irradiated path by immunofluorescence (Figs. 2*A*, 1–5). Immunostaining with anti-HMGN1 discriminated between the *Hmgn1*$^{-/-}$ cells, lacking the protein (*asterisks*), and the *Hmgn1*$^{+/+}$ cells (*arrows*), which stained brightly (Fig. 2*A*). Within 10 minutes after irradiation, phosphorylated H2AX accumulated in the irradiated path in both *Hmgn1*$^{+/+}$ and *Hmgn1*$^{-/-}$ cells (Figs. 2*A*, 3). Western analysis with histones extracted from either *Hmgn1*$^{+/+}$ or *Hmgn1*$^{-/-}$ cells 5 minutes after irradiation with 0.6 Gy (inserts Figs. 2*A*, 3) confirmed that the γ-H2AX levels were similar in both cell types. Therefore, we conclude that HMGN1 does not affect significantly the ionizing radiation–induced generation of γ-H2AX, a result that is in agreement with recent findings that H2AX phosphorylation does not constitute the primary signal for the accumulation of repair complexes at damaged chromatin sites (27).

Because hypersensitivity to ionizing radiation has been linked to aneuploidy and other chromosome abnormalities, we carried out chromosome analysis in mitotic spreads of *Hmgn1*$^{+/+}$ and *Hmgn1*$^{-/-}$ cells. These cytogenetic analyses did not reveal major differences between the two cell types; an indication that loss of HMGN1 protein does not lead to significant genomic instability (not shown).

Ionizing radiation treatment is known to activate the G_2-M cell cycle checkpoint, presumably to allow the DNA repair machinery to repair the DNA damage before entering mitosis (5, 13). FACS analysis of propidium iodide–stained cells, which were exposed to various doses of ionizing radiation (0.6–6 Gy), did not reveal major differences between the cell cycle profiles of *Hmgn1*$^{+/+}$ and *Hmgn1*$^{-/-}$ MEFs (Fig. 2*B*). Thus, HMGN1 protein did not have major effects on the proportion of cells in S, G_2-M, and G_1. However, when the entry into mitosis was specifically examined, by FACS analysis of cells stained with antibodies to phosphorylated Ser10 in H3, we noticed ionizing radiation dose-dependent differences between *Hmgn1*$^{+/+}$ and *Hmgn1*$^{-/-}$ MEFs (Fig. 3*A*). Thus, 1 hour after irradiation with 0.6 Gy, the number of *Hmgn1*$^{+/+}$ cells in mitosis was 70% lower than that of nonirradiated cells. In contrast, an identical dose of ionizing radiation treatment did not affect the mitotic entry of *Hmgn1*$^{-/-}$ cells, which showed the same number of cells in mitosis before and after irradiation (Fig. 3*A*). With increasing dose of irradiation, the differences between the wild-type and knockout cells gradually decrease and when irradiated with 6 Gy there was no difference between the two cell types. Similar results ere obtained with transformed MEFs (Fig. 3*B*). Significantly, Dox-induced expression of wild-type HMGN1 (Fig. 3*C*), but not of the S20,24E-HMGN1 mutant (Fig. 3*D*), restored the G_2-M checkpoint. Just like wild-type cells, *Hmgn1*$^{-/-}$ MEFs expressing HMGN1 arrested their mitotic entry even at low ionizing radiation doses. These results indicate that loss of the interaction of HMGN1 with chromatin in the *Hmgn1*$^{-/-}$ cells alters the G_2-M checkpoint, and at low ionizing radiation doses these cells enter mitosis without pausing.

Increased tumor burden in *Hmgn1*$^{-/-}$ mice

Aberrant regulation of cell-cycle checkpoints impairs DNA-damage repair processes (5, 13). Faulty repair may ultimately lead to the accumulation of mutations and increased incidence of tumors. Therefore, the HMGN1-related aberrant activation of the G_2-M checkpoint may increase the tumor frequency not only in irradiated, but even in untreated *Hmgn1*$^{-/-}$ mice. Indeed, longevity studies of *Hmgn1*$^{+/+}$ or *Hmgn1*$^{-/-}$ animals indicated a greater tumor burden in mice lacking HMGN1 protein (Table 1). The increase was attributable mainly to a greater number of animals with multiple malignant tumors. Thus, over 40% of the *Hmgn1*$^{-/-}$ mice had multiple tumors compared with only 17% of the male and 27% of the female *Hmgn1*$^{+/+}$ animals. Likewise, 58% of the males and 82% of the female *Hmgn1*$^{-/-}$ mice, but only 29% and 55% of the wild-type male and female mice, had malignant tumors. Whereas none of the male *Hmgn1*$^{+/+}$ animals developed metastasis, 25% of the male *Hmgn1*$^{-/-}$ mice had malignant tumors that metastasized. Loss of HMGN1 protein did not affect the life span of the mice or the average age at which the tumor was detected. For male *Hmgn1*$^{+/+}$ and *Hmgn1*$^{-/-}$ mice, the average age at which the tumor was detected was 81 and 82 weeks, respectively, whereas for the female *Hmgn1*$^{+/+}$ and *Hmgn1*$^{-/-}$ mice it was 88 and 86 weeks. However, in mice that died young, tumors were detected at significantly younger ages in *Hmgn1*$^{-/-}$ mice. Within 57 weeks of birth, 4 *Hmgn1*$^{+/+}$ and 13 *Hmgn1*$^{-/-}$ died; none of the *Hmgn1*$^{+/+}$ mice but five (38%) of the *Hmgn1*$^{-/-}$ mice developed tumors. In addition, loss of HMGN1 led to an increase in the frequency of endocrine malignancies including adrenal pheochromocytoma, which, although of low incidence, were observed only in *Hmgn1*$^{-/-}$ animals. Loss of HMGN1 also lead to marginal increase in incidence of hematopoietic neoplasms, hepatic neoplasms, and hemangiosarcomas, and a few unusual tumors were noted only in the *Hmgn1*$^{-/-}$ mice: granular cell tumor of the brain (one *Hmgn1*$^{-/-}$ female); jejunal carcinoma (one *Hmgn1*$^{-/-}$ female); and renal tubule neoplasm (3 *Hmgn1*$^{-/-}$ males; Table 1).

The increased tumor burden of *Hmgn1*$^{-/-}$ mice is most obvious when all the differences between the wild-type and knockout mice are combined: The tumor burden of mice lacking HMGN1 protein is almost 2-fold higher than that of wild-type mice (Fig. 4). The *P* values,

using the two-sided Fisher test, were 0.35 for the total animals with tumors, 0.014 for total malignant tumors, 0.4 for malignant tumors with metastasis, and 0.2 for total malignant tumors. In the statistical test, we grouped the *Hmgn1*$^{-/-}$ males and females into one group and the *Hmgn1*$^{+/+}$ males and females into another group. The values obtained were similar to those when each sex was compared between the two types of mice. The relative low number of animals precluded more reliable statistical values; however, we note that all the comparisons had the same tendency: The tumor burden of the mice lacking HMGN1 was higher than in their wild-type littermates. The most significant difference was in the incidence of total malignant tumors that was significantly higher in the *Hmgn1*$^{-/-}$ mice (P = 0.014). In addition, none of the 24 male *Hmgn1*$^{+/+}$ mice, but 6 of the male *Hmgn1*$^{-/-}$ mice (P = 0.026), had metastatic malignant tumors.

Tumorigenic potential of *Hmgn1*$^{-/-}$ mouse embryonic fibroblasts

The increased incidence of spontaneous and more aggressive tumors in *Hmgn1*$^{-/-}$ mice raises the possibility that loss of HMGN1 protein confers tumorigenic potential to the cells. Indeed, both primary and transformed MEFs generated form *Hmgn1*$^{-/-}$ embryos had a faster growth rate, with a doubling time of 12 hours, whereas MEFs generated from their *Hmgn1*$^{+/+}$ littermates grew slower with a doubling time of 19 hours (Fig. 5*A* and *B*). Furthermore, whereas the *Hmgn1*$^{+/+}$ MEFs senesce and stop growing by passage 8, the *Hmgn1*$^{-/-}$ MEFs proliferate efficiently at this passage and reached senescence only at passage 13 (not shown). In the soft agar colony growth assay, transformed *Hmgn1*$^{-/-}$ MEFs grew more efficiently and formed more colonies than transformed *Hmgn1*$^{+/+}$ MEFs. When plated on soft agar, 83% of transformed *Hmgn1*$^{-/-}$ MEFs, but only 24% of the transformed *Hmgn1*$^{+/+}$ MEFs formed colonies (Fig. 5*C*). Nontransformed MEFs did not grow and did not form colonies.

Injection of the transformed *Hmgn1*$^{-/-}$ and *Hmgn1*$^{+/+}$ MEFs into immunodeficient nude mice indicates that loss of HMGN1 increased the *in vivo* tumorigenic properties of the cells. Within 25 days, 56% of the nude mice that were injected with *Hmgn1*$^{-/-}$ MEFs, but only 10% of the animals that were injected with the same amount of *Hmgn1*$^{+/+}$ MEFs, developed tumors (Fig. 5*C*). The average tumor size developed in the mice injected with *Hmgn1*$^{-/-}$ MEFs was four times larger than the tumor developed after injection of *Hmgn1*$^{+/+}$ MEFs cells. Taken together, these observations indicate an increased tumorigenic potential in cells lacking HMGN1 protein.

Discussion

It is now well established that chromatin plays a central role in the cellular response to ionizing radiation and in DSB repair (1, 28). Here, we show that HMGN1, a structural protein known to affect chromatin condensation (14) and histone modifications (26), plays a role in the ionizing radiation response. The link between HMGN1 and the ionizing radiation response is supported by several observations: First, the survival of ionizing radiation–treated *Hmgn1*$^{-/-}$ mice is lower than that of their *Hmgn1*$^{+/+}$ littermates; second, *Hmgn1*$^{-/-}$ MEFs are more sensitive to ionizing radiation than *Hmgn1*$^{+/+}$ MEFs; and third, expression of HMGN1, but not S20,24E-HMGN1 mutant protein, in *Hmgn1*$^{-/-}$ MEFs increases their ionizing radiation resistance. Thus, HMGN1 can be considered as an additional chromatin binding protein that affects the repair of DSBs.

DSB repair involves changes in chromatin structure and in posttranslational modifications in histone tails (1, 8, 28). HMGN1 affects both the levels of histone posttranslational modification (26) and the stability of the higher-order chromatin structure (14) and, therefore, it could affect one or more key steps in the DSB repair processes. The phosphorylation of H2ax at and near DSBs triggers the accumulation of various types of

histone modifications that lead to changes in chromatin condensation that are necessary for subsequent DSB repair (28, 29). Although we have not detected significant differences in the levels of γ-H2AX between *Hmgn1*$^{+/+}$ and *Hmgn1*$^{-/-}$ cells, loss of HMGN1 could affect some of the other histone modifications associated with DSB repair (28). It may be relevant that in both *H2ax*$^{-/-}$ (30) and *Hmgn1*$^{-/-}$ (Fig. 3) cells, the G_2-M checkpoint is impaired. Both of these cells were less sensitive to ionizing radiation treatment and exhibited a significantly higher threshold than normal, before a significant number of cells arrested before entry into M. For the *H2ax*$^{-/-}$ cells, it was proposed that below a certain threshold of DNA damage, lack of H2AX phosphorylation disrupts the accumulation of factors necessary to activate the G_2-M checkpoint. Just like H2AX, HMGN1 may be necessary to efficiently activate the G_2-M threshold at low, but not at high, levels of DSB (30). The failure of both *H2ax*$^{-/-}$ and *Hmgn1*$^{-/-}$ cells to activate the G_2-M checkpoint at low ionizing radiation doses strengthens the notion that the structure of chromatin plays an important role in this process. However, the phenotype of the two cell types is distinct in many aspects, indicating distinct ionizing radiation response pathways involving chromatin structure. We suggest that HMGN1, and perhaps other members of the HMGN protein family, facilitate the formation of the chromatin structures that ensure efficient ionizing radiation response and proper DSB repair.

Our finding that the tumor incidence of aged mice lacking HMGN1 protein is almost twice that of wild-type mice is in agreement with a possible role for the protein in ensuring the fidelity of the G_2-M checkpoint. The G_2-M checkpoint arrest of ionizing radiation–irradiated cells serves to ensure the fidelity of DSB repair before entry into mitosis (13, 31). Faulty repair may lead to mutation and increase tumor frequency. Cells taken from aged mice have significantly more DSBs than cells taken from young mice, an indication of spontaneous DSB occurrences during their life span (32). Thus, faulty G_2-M arrest and increased mutation frequency could be the underlying cause for the increased tumor burden in *Hmgn1*$^{-/-}$ mice. Because HMGN1 is expressed in most tissues, it can be expected that the tumors would be found in various tissues.

Primary mouse cells usually require introduction of two “activated” oncogenes for transformation, unless certain key growth control or oncogenic genes are already disrupted (33, 34). Our finding that a single transformation with SV40 large T antigen was sufficient to change the basic properties of the primary cells indicate that the absence of HMGN1 is sufficient to disrupt cellular events that control cell proliferation and growth. The growth control mechanisms disrupted by loss of HMGN1 protein may have rendered the animals and the MEFs more susceptible to additional events that ultimately lead to malignant transformations. The interaction of HMGN1 protein with nucleosomes alters the structure of chromatin and modulates various DNA-related nuclear processes including transcription (18–20). Thus, the increased tumor burden and tumorigenicity of *Hmgn1*$^{-/-}$ mice and MEFs could be due not only to an impaired G_2-M checkpoint but also to indirect effects that lead to alteration in the cellular transcription profile.

Our findings reemphasize the importance of chromatin in the cellular response to ionizing radiation damage and identify HMGN1 as an additional chromatin regulatory element involved in carcinogenesis.

Acknowledgments

Grant support: Federal funds from the National Cancer Institute under contract NO1-CO-12400 to Science Applications International Corporation-Frederick.

The costs of publication of this article were defrayed in part by the payment of page charges. This article must therefore be hereby marked *advertisement* in accordance with 18 U.S.C. Section 1734 solely to indicate this fact.

We thank S.H. Garfield and S. Wincovitch [Confocal Core Facility, Laboratory of Experimental Carcinogenesis, Center for Cancer Research, National Cancer Institute (NCI)] for help with confocal microscopy and UV scissor experiments, Drs. K. Kraemer and H. Tonoli (NCI) for critical review of the manuscript, Drs. O. Sedelnikova and W.M Bonner (NCI) for advice, Dr. J. Ward for examination of the irradiated mice, and Amy Chen (Transgenic Core Facility, National Human Genome Research Institute) for help in generating the *Hmgn1*$^{-/-}$ mice.

References

1. Peterson CL, Cote J. Cellular machineries for chromosomal DNA repair. Genes Dev. 2004; 18:602–6. [PubMed: 15075289]
2. Redon C, Pilch D, Rogakou E, Sedelnikova O, Newrock K, Bonner W. Histone H2A variants H2AX and H2AZ. Curr Opin Genet Dev. 2002; 12:162–9. [PubMed: 11893489]
3. Celeste A, Difilippantonio S, Difilippantonio MJ, et al. H2AX haploinsufficiency modifies genomic stability and tumor susceptibility. Cell. 2003; 114:371–83. [PubMed: 12914701]
4. Bassing CH, Suh H, Ferguson DO, et al. Histone H2AX: a dosage-dependent suppressor of oncogenic translocations and tumors. Cell. 2003; 114:359–70. [PubMed: 12914700]
5. Marks PA, Richon VM, Breslow R, Rifkind RA. Histone deacetylase inhibitors as new cancer drugs. Curr Opin Oncol. 2001; 13:477–83. [PubMed: 11673688]
6. Espinosa JM, Emerson BM. Transcriptional regulation by p53 through intrinsic DNA/chromatin binding and site-directed cofactor recruitment. Mol Cell. 2001; 8:57–69. [PubMed: 11511360]
7. Klochendler-Yeivin A, Muchardt C, Yaniv M. SWI/SNF chromatin remodeling and cancer. Curr Opin Genet Dev. 2002; 12:73–9. [PubMed: 11790558]
8. Bakkenist CJ, Kastan MB. DNA damage activates ATM through intermolecular autophosphorylation and dimer dissociation. Nature. 2003; 421:499–506. [PubMed: 12556884]
9. Shiloh Y. ATM and related protein kinases: safeguarding genome integrity. Nat Rev Cancer. 2003; 3:155–68. [PubMed: 12612651]
10. Green CM, Almouzni G. When repair meets chromatin: first in series on chromatin dynamics. EMBO Rep. 2002; 3:28–33. [PubMed: 11799057]
11. Smerdon MJ, Conconi A. Modulation of DNA damage and DNA repair in chromatin. Prog Nucleic Acid Res Mol Biol. 1999; 62:227–55. [PubMed: 9932456]
12. Thoma F. Light and dark in chromatin repair: repair of UV-induced DNA lesions by photolyase and nucleotide excision repair. EMBO J. 1999; 18:6585–98. [PubMed: 10581233]
13. Kastan MB, Bartek J. Cell-cycle checkpoints and cancer. Nature. 2004; 432:316–23. [PubMed: 15549093]
14. Bustin M. Chromatin unfolding and activation by HMGN(*) chromosomal proteins. Trends Biochem Sci. 2001; 26:431–7. [PubMed: 11440855]
15. Bustin M. Regulation of DNA-dependent activities by the functional motifs of the high-mobility-group chromosomal proteins. Mol Cell Biol. 1999; 19:5237–46. [PubMed: 10409715]
16. Catez F, Brown DT, Misteli T, Bustin M. Competition between histone H1 and HMGN proteins for chromatin binding sites. EMBO Rep. 2002; 3:760–6. [PubMed: 12151335]
17. Phair RD, Misteli T. High mobility of proteins in the mammalian cell nucleus. Nature. 2000; 404:604–9. [PubMed: 10766243]
18. Ding HF, Rimsky S, Batson SC, Bustin M, Hansen U. Stimulation of RNA polymerase II elongation by chromosmal protein HMG-14. Science. 1994; 265:796–9. [PubMed: 8047885]
19. Trieschmann L, Alfonso PJ, Crippa MP, Wolffe AP, Bustin M. Incorporation of chromosomal proteins HMG-14/-17 into nascent nucleosomes induces an extended chromatin conformation and enhances the utilization of active transcription complexes. EMBO J. 1995; 14:1478–89. [PubMed: 7729423]
20. Paranjape SM, Krumm A, Kadonaga JT. HMG17 is a chromatin-specific transcriptional coactivator that increases the efficiency of transcription initiation. Genes Dev. 1995; 9:1978–91. [PubMed: 7649479]
21. Vestner B, Bustin M, Gruss C. Stimulation of replication efficiency of a chromatin template by chromosomal protein HMG-17. J Biol Chem. 1998; 273:9409–14. [PubMed: 9545265]

22. Birger Y, West KL, Postnikov YV, et al. Chromosomal protein HMGN1 enhances the rate of DNA repair in chromatin. EMBO J. 2003; 22:1665–75. [PubMed: 12660172]
23. Rogakou EP, Boon C, Redon C, Bonner WM. Megabase chromatin domains involved in DNA double-strand breaks *in vivo*. J Cell Biol. 1999; 146:905–16. [PubMed: 10477747]
24. Celeste A, Petersen S, Romanienko PJ, et al. Genomic instability in mice lacking histone H2AX. Science. 2002; 296:922–7. [PubMed: 11934988]
25. Prymakowska-Bosak M, Misteli T, Herrera JE, et al. Mitotic phosphorylation prevents the binding of HMGN proteins to chromatin. Mol Cell Biol. 200; 21:5169–78. [PubMed: 11438671]
26. Lim JH, Catez F, Birger Y, et al. Chromosomal protein HMGN1 modulates histone H3 phosphorylation. Mol Cell. 2004; 15:573–84. [PubMed: 15327773]
27. Celeste A, Fernandez-Capetillo O, Kruhlak MJ, et al. Histone H2AX phosphorylation is dispensable for the initial recognition of DNA breaks. Nat Cell Biol. 2003; 5:675–9. [PubMed: 12792649]
28. Fernandez-Capetillo O, Nussenzweig A. Linking histone deacetylation with the repair of DNA breaks. Proc Natl Acad Sci U S A. 2004; 101:1427–8. [PubMed: 14757822]
29. Fernandez-Capetillo O, Allis CD, Nussenzweig A. Phosphorylation of histone H2B at DNA double-strand breaks. J Exp Med. 2004; 199:1671–7. [PubMed: 15197225]
30. Fernandez-Capetillo O, Chen HT, Celeste A, et al. DNA damage-induced G_2-M checkpoint activation by histone H2AX and 53BP1. Nat Cell Biol. 2002; 4:993–7. [PubMed: 12447390]
31. Zhou BB, Elledge SJ. The DNA damage response: putting checkpoints in perspective. Nature. 2000; 408:433–9. [PubMed: 11100718]
32. Sedelnikova OA, Horikawa I, Zimonjic DB, Popescu NC, Bonner WM, Barrett JC. Senescing human cells and ageing mice accumulate DNA lesions with unrepairable double-strand breaks. Nat Cell Biol. 2004; 6:168–70. [PubMed: 14755273]
33. Kamijo T, Zindy F, Roussel MF, et al. Tumor suppression at the mouse INK4a locus mediated by the alternative reading frame product p19ARF. Cell. 1997; 91:649–59. [PubMed: 9393858]
34. Hollander MC, Fornace AJ Jr. Genomic instability, centrosome amplification, cell cycle checkpoints and Gadd45a. Oncogene. 2002; 21:6228–33. [PubMed: 12214253]

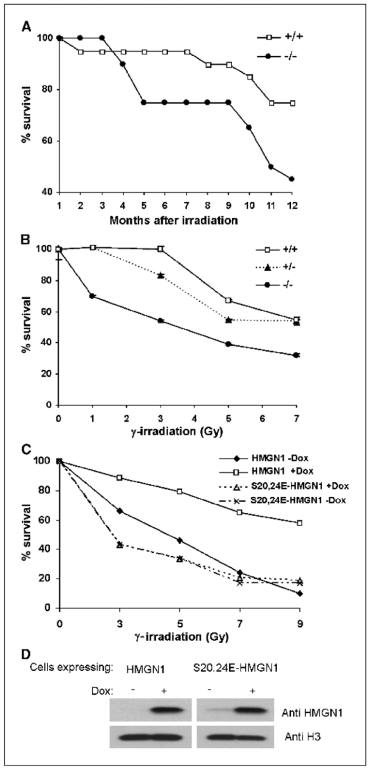

Figure 1.

Increased sensitivity to ionizing radiation upon loss of chromosomal protein HMGN1. *A*, decreased survival of *Hmgn1*$^{-/-}$ mice. Shown is a plot of the survival of *Hmgn1*$^{-/-}$ and *Hmgn1*$^{+/+}$ mice treated according to the ionizing radiation protocol described in Materials and Methods. *B*, decreased survival of *Hmgn1*$^{-/-}$ and *Hmgn1*$^{-/+}$ MEFs. Shown is the survival of cells 72 hours after γ-irradiation with the indicate doses. *C*, rescue of ionizing radiation hypersensitivity by reexpression of wild-type, but not mutant, HMGN1 protein. HMGN1 indicate cells that express wild-type HMGN1 protein when exposed to Dox (+*Dox*) but do not express the protein in the absence of Dox (−*Dox*). S20,24E-HMGN1 indicates cells that either express or do not express this mutant, which does not bind to chromatin. Note that only the expression of wild-type HMGN1 protein enhances the ability of the *Hmgn1*$^{-/-}$ cells to survive ionizing radiation treatment. Note the small error bars in (*B*). Data in (*C*) are average of two repeats. *D*, Western blot analysis of cells that express either wild-type HMGN1 or the S20,24E-HMGN1 mutant protein under the Dox-inducible promoter. Note that addition of Dox induced protein expression. Anti-histone H3 serves as loading control.

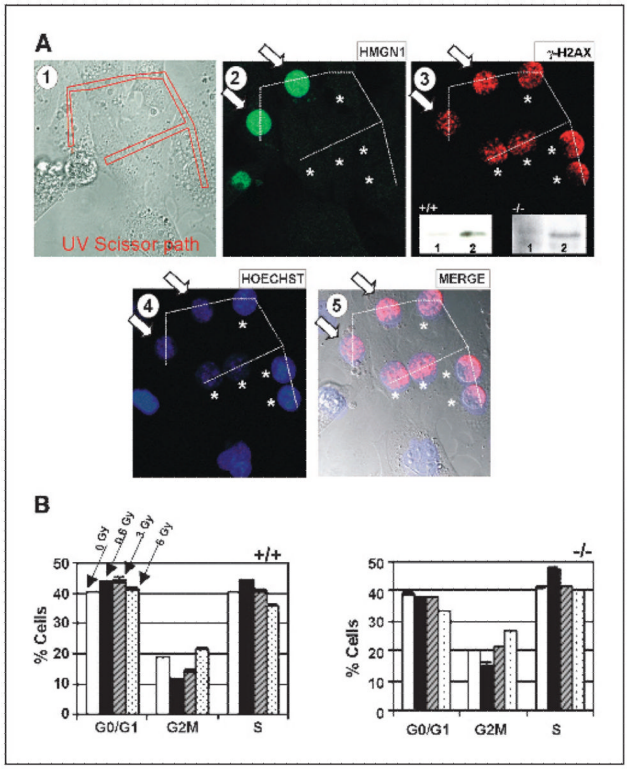

Figure 2.

Unaltered H2AX phosphorylation and cell cycle in *Hmgn1*$^{-/-}$ MEFs. A, γ-H2AX generation. A mixture of *Hmgn1*$^{+/+}$ and *Hmgn1*$^{-/-}$ MEFs was exposed to UV laser along a defined path and immunostained with the antibodies indicated on top of the panels. Asterisks point to *Hmgn1*$^{-/-}$ cells, arrows to *Hmgn1*$^{+/+}$ cells. *1*, phase contrast. *2*, immunostaining for HMGN1. *3*, immunostaining for γ-H2AX. Inserts in the bottom depict Western blots (anti–γ-H2Ax) of histones extracted from either *Hmgn1*$^{+/+}$ (*left*) or *Hmgn1*$^{-/-}$ (*right*) cells before (*lane 1*) and 5 minutes after irradiation with 0.6 Gy (*lane 2*). *4*, nuclei staining with Hoechst. *5*, overlay of (*1*) to (*4*). Note that γ-H2AX staining follows strictly the path irradiation laser. *B*, loss of HMGN1 does not affect cell cycle progression. FACS analysis of *Hmgn1*$^{-/-}$ and *Hmgn1*$^{+/+}$ cells exposed to the ionizing radiation doses indicated by the legend above the first column set. *Bars*, SD of triplicate experiments.

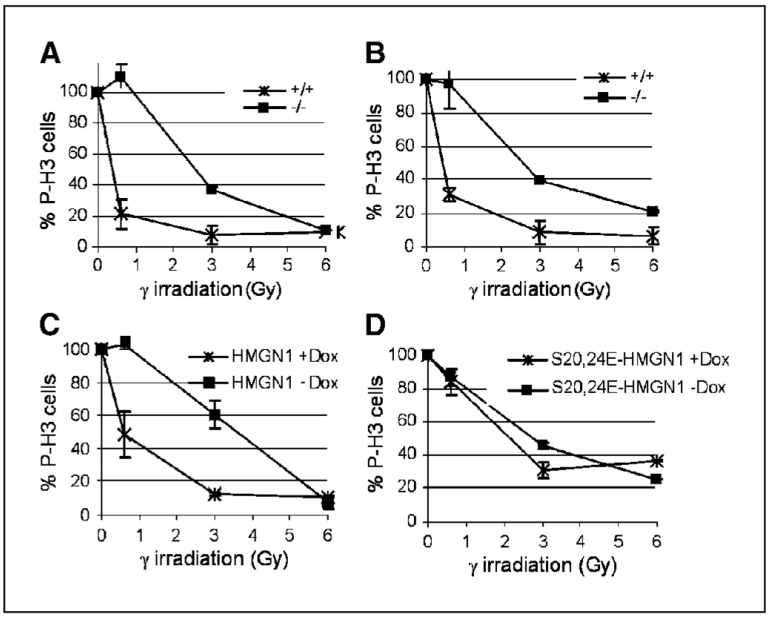

Figure 3.

HMGN1 affects the G_2-M checkpoint. Shown are the percentage of mitotic cells, determined by staining with anti–phosho-H3 after exposure to various doses of γ-irradiation. *A*, primary MEFs. *B*, transformed MEFs. *C*, revertant MEFs either expressing (+*Dox*) or not expressing (−*Dox*) wild-type HMGN1. *D*, revertant MEFs either expressing (+*Dox*) or not expressing (−*Dox*) the S20,24E HMGN1 mutant (which does not bind to chromatin). On the *Y* axis, the number of P-H3–positive cells in nonirradiated cultures is set to 100%.

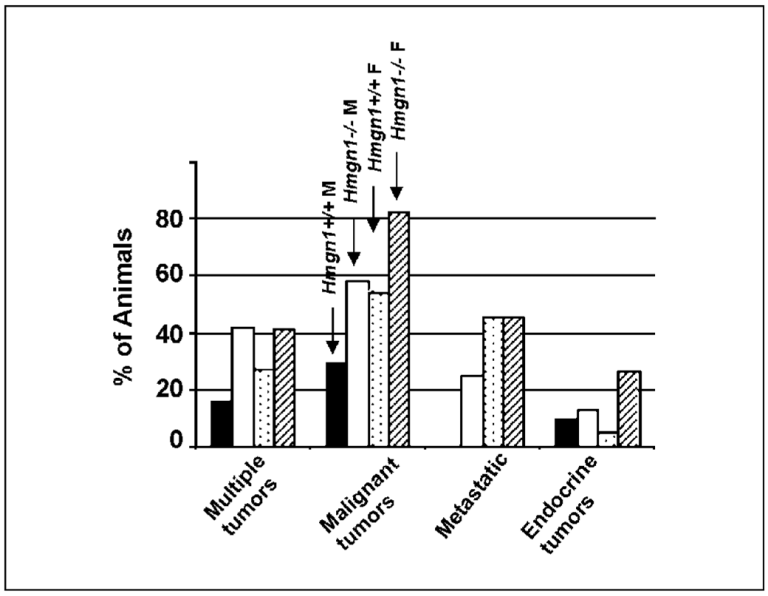

Figure 4.

Increased tumor incidence in *Hmgn1*$^{-/-}$ mice. Classification of tumors is from Table 1. The legend above the central columns identifies the genotype and the sex (*M*, male; *F*, female) of the mice. In mice that died young, tumors were detected at significantly younger ages in *Hmgn1*$^{-/-}$ mice. Within 57 weeks of birth, 4 *Hmgn1*$^{+/+}$ and 13 *Hmgn1*$^{-/-}$ died; none of the Hmgn1$^{+/+}$ mice but 5 (38%) of the *Hmgn1*$^{-/-}$ mice developed tumors. Statistical *P* values were given in the text.

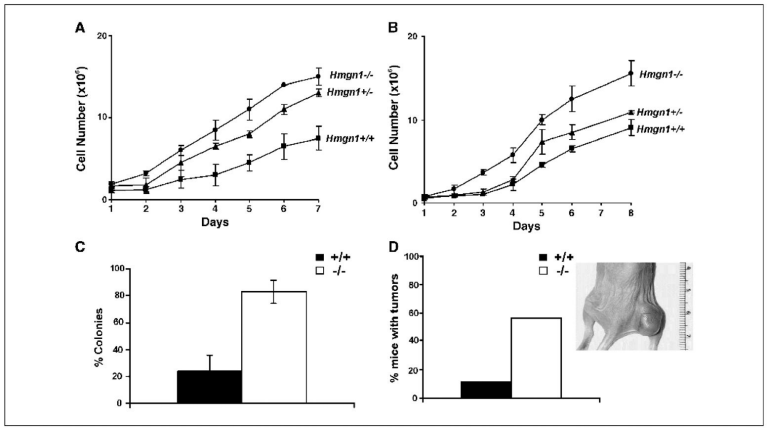

Figure 5.

Increased tumorigenic potential in *Hmgn1*$^{-/-}$ MEFs. *A*, increased proliferation rate of MEFs prepared from *Hmgn1*$^{-/-}$, *Hmgn1*$^{+/-}$, or *Hmgn1*$^{+/+}$ embryos. *B*, increased proliferation rate of transformed *Hmgn1*$^{-/-}$ and Hmgn1$^{+/-}$ MEFs. *C*, increased colony formation in soft agar by *Hmgn1*$^{-/-}$ MEFs. *D*, increased generation of tumors in Nu/Nu mice by *Hmgn1*$^{-/-}$ MEFs. SD was derived from at least three experiments of triplicate cell dishes (*A* and *B*) or two experiments of triplicates (*C*). (*D*) was repeated twice.

Table 1

Type and location of spontaneous tumors in *Hmgn1*$^{-/-}$ and *Hmgn1*$^{+/+}$ mice

	***Hmgn1*$^{+/+}$ male**	***Hmgn1*$^{-/-}$ male**	***Hmgn1*$^{+/+}$ female**	***Hmgn1*$^{-/-}$ female**
No. animals	24	24	22	22
Total no. tumors	19	31	28	30
Total animals with tumors [*]	13	15	18	17
Total animals with multiple tumors (%)	4 (17)	10 **(42)** [†]	6 (27)	9 **(41)**
Total animals with malignant tumors (%)	7 (29)	14 **(58)**	12 (55)	18 **(82)**
Total animals with metastasis (%)	0 (0)	6 **(25)**	10 (45)	10 (45)
Brain				
Granular cell tumor	0	0	0	1
Harderian gland				
Adenoma	5	4	4	3
Carcinoma	1	0	0	0
Hematopoietic neoplasm				
Histocytic sarcoma	0	1	3	4
Marginal zone lymphoma	1	1	0	1
B-cell lymphoma	0	2	7	6
T-cell lymphoma	0	1	0	0
Total animals with hematopoietic neoplasms (%) [‡]	1 (4)	4 **(17)**	10 (45)	11 (50)
Jejunum-carcinoma	0	0	0	1
Kidney				
Carcinoma	0	2	0	0
Adenoma	0	2	0	0
Total animals with kidney tumors (%) [§]	0	3 **(13)**	0	0
Liver				
Adenoma, hepatocellular	1	5	2	0
Hepatoblastoma	1	0	0	0
Carcinoma, hepatocellular	2	0	0	0
Total animals with liver tumors (%)	2 (8)	5 **(21)**	2 (11)	0
Lung				
Adenoma, alveolar	3	2	4	4
Carcinoma, alveolar	2	3	1	2
Total animals with lung tumors (%)	5 (21)	5 (21)	5 (23)	6 (27)
Pancreas				
Adenoma, acinar cell (%)	0	1 (4)	1 (5)	0
Skin				
Adenoma, sebaceous gland	1	0	0	0
Sarcoma, tail	0	1	0	0
Uterus				
Hemangiosarcoma	NA	NA	0	1

	***Hmgn1*$^{+/+}$ male**	***Hmgn1*$^{-/-}$ male**	***Hmgn1*$^{+/+}$ female**	***Hmgn1*$^{-/-}$ female**
Hemangioma	NA	NA	1	0
Cervix leiomyosarcoma	NA	NA	1	0
Hemangiosarcomas (other tissues)	0	3	0	1
Endocrine neoplasms				
Adrenal-pheochromocytoma	0	1	0	2
Pituitary adenoma, pars distalis	1	0	2	0
Thyroid-adenoma, follicle	1	2	1	2
Ovary granulosa cell tumor	NA	NA	0	2
Total animals with endocrine tumors (%)	2 (8)	3 (13)	3 (14)	6 (27)

Abbreviation: NA, not applicable.

[*] In mice that died young, tumors were detected at significantly younger ages in *Hmgn1*$^{-/-}$ mice. Within 57 weeks of birth, 4 *Hmgn1*$^{+/+}$ and 13 *Hmgn1*$^{-/-}$ died; none of the *Hmgn1*$^{+/+}$ mice but 5 (38%) of the *Hmgn1*$^{-/-}$ mice developed tumors.

[†] The values indicated in bold are deemed biologically significant differences between wild-type and Ko mice.

[‡] Some animals had more than one type of tumor.

[§] One animal had both tumor types.